

Coherent-nuclear pion photoproduction and neutron radii

Gerald A. Miller *University of Washington, Seattle, Washington 98195-1560, USA*

(Received 6 August 2019; published 14 October 2019)

Background: Knowing the difference between the neutron and proton densities of nuclei is a significant topic because of its importance for understanding neutron star structures and cooling mechanisms. The coherent-nuclear photoproduction of pions, (γ, π^0), combined with elastic electron scattering, has been suggested to be a very accurate probe of density differences.

Purpose: Study the (γ, π^0) reaction mechanism so as to better access the uncertainties involved in extracting the neutron density.

Methods: Include the effects of final-state pion-nucleus charge-exchange reactions on the cross section and study the influence of the nonzero spatial extent of the proton.

Results: The effects of final-state charge-exchange increase the cross section between 6% and 5%, generally decreasing as the momentum transfer increases. This leads to an increase of the extracted neutron skin distance by about 50%. The validity of the previous treatments of the proton size is confirmed.

Conclusion: The model dependence of the theoretically computed cross section increases the total systematic uncertainty (experiment plus theory) in extracting the neutron skin from the (γ, π^0) cross section by at least a factor of three.

DOI: [10.1103/PhysRevC.100.044608](https://doi.org/10.1103/PhysRevC.100.044608)

I. INTRODUCTION

A recent letter [1] “establishes the coherent photoproduction of π^0 mesons from ^{208}Pb as an accurate probe of the nuclear shape, which has sufficient sensitivity to detect and characterize the neutron skin.” The neutron skin is the difference between the neutron and proton densities. That work uses one specific theoretical model to determine the neutron skin thickness to be 0.15 ± 0.03 (stat.) $^{+0.02}_{-0.03}$ (sys.) fm. Reference [1] also points out that the nature of the neutron skin is important for understanding neutron star structure and cooling mechanisms [2–6], searches for physics beyond the standard model [7,8], the nature of three-body forces in nuclei [9,10], collective nuclear excitations [11–14], and flows in heavy-ion collisions [15,16]. A nice summary of the relation between nuclear and neutron star physics is provided in Ref. [17].

As a result, it is important to understand the theoretical model dependence in computing π^0 coherent photoproduction cross section in full detail. Reference [1] analyzed its data using the elegant nuclear reaction theory of Ref. [18] based on the unitary isobar model [19] for photoproduction on a free proton. This model gave good agreement with early, less-precise data on several different nuclei [20,21]. Possible systematic errors in the theory were not included in the analysis [1] that obtained the neutron skin. One may worry that any systematic error in the theory might have an effect on the extracted skin that is comparable to, or larger than, the reported systematic error. It is also worth mentioning that alternate reaction theories exist, see, e.g., Ref. [22]. Therefore it is responsible to examine whether or not any possible updates

are relevant. In particular, effects that are usually ignorable may become relevant given the reported [1] extraordinarily high precision of $^{+0.02}_{-0.03}$ fm.

The aim here is only to study the possible systematic effects that enter from uncertainties in the reaction theory. Finding a better way to extract the neutron skin from the reaction is a topic that is beyond the scope of this paper. Further, it shall be argued that a variety of contributions to the systematic error in the theory make that total systematic uncertainty much larger than ones originating from experiments.

The present focus is on the energy range of photon energies between 180 and 190 MeV where the effects of the pion-nucleus optical potential are very small so that the outgoing pions can be treated in plane-wave approximation. Even so, in this energy range the (γ, π^0) reaction proceeds through the excitation of an intermediate Δ [1,20,21]. The present note is concerned with two effects that might lead to a systematic error in the theory. The first is the effect of production of a charged pion followed by a final-state charge exchange reaction leading to the production of a π^0 while leaving the nucleus in its ground state. The relevant diagrams are shown in Fig. 1. The impulse approximation of Fig. 1(a) is discussed in Sec. II.

As explained in the textbook by Ericson and Weise [23], the processes of Fig. 1(b) are dominant for photoproduction near threshold [24,25]. Moreover, Wilhelm and Arenhövel [26] studied the effect of final-state charge exchange in the region of the Delta (Δ) resonance and found that it causes a significant increase in the computed cross section. Therefore it is necessary to examine the effects of charge exchange. These are not included in the pion-nucleus optical potential [27]

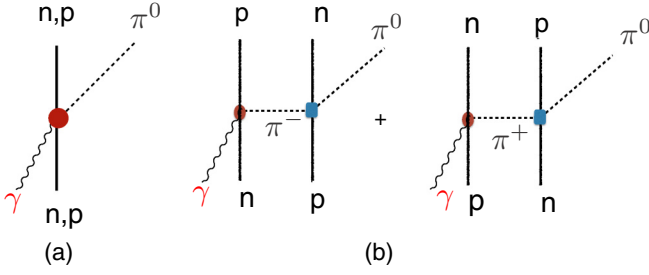


FIG. 1. (a) One-body mechanism, impulse approximation. (b) Two-body mechanism, production of charged pion followed by charge exchange on a second nucleon.

used in Ref. [18]. However, final-state pion-nucleon charge exchange is part of the model [19] for π^0 production on a nucleon [28], and therefore must be included in the nuclear calculation. This effect is discussed in Sec. III.

The influence of the nonzero spatial extent of the proton, a subject of much current interest, is the second effect examined here. See the reviews [29,30]. The radius of the proton is much larger than 0.03 fm, so this effect bears close scrutiny as has been pointed out already in Ref. [31]. This effect is discussed in Sec. IV. Section V is concerned with the numerical results, and a summary and discussion is presented in Sec. VI.

II. ONE-BODY MECHANISM

The dominant one-body (impulse approximation) term is shown in Fig. 1(a). The spin-averaged amplitude for production on a single nucleon, in the notation of Ericson and Weise [23], is given by

$$O^{IA} = \frac{4A^{(3/2)}}{9} \hat{\mathbf{q}}_{cN} \cdot (\hat{\mathbf{k}}_{cN} \times \boldsymbol{\epsilon}), \quad (1)$$

in which the incoming photon has momentum k , and the outgoing π^0 has momentum q in the photon-nucleus center-of-mass (CM) frame. The subscript cN denotes evaluation in the photon-nucleon CM frame with the transformation from the laboratory frame given in Ref. [18]. The photon transverse polarization is denoted by $\boldsymbol{\epsilon}$, the photoproduction amplitude for the Δ mechanism is written as $A^{(3/2)}$ and the spin-flip term is ignored because the ^{208}Pb ground state has no spin. The resulting nuclear amplitude is given by

$$\begin{aligned} \langle A | O^{IA} | A \rangle &= \frac{4A^{(3/2)}}{9} \hat{\mathbf{q}}_{cN} \cdot (\hat{\mathbf{k}}_{cN} \times \boldsymbol{\epsilon}) \\ &\times \int d^3r [\rho_n(\mathbf{r}) + \rho_p(\mathbf{r})] e^{i(\mathbf{k}-\mathbf{q}) \cdot \mathbf{r}}, \end{aligned} \quad (2)$$

where \mathbf{k} is the photon momentum in the laboratory, \mathbf{q} is the pion momentum, and the neutron (n) and proton (p) densities are given by $\rho_{n,p}(\mathbf{r})$. It is worthwhile to display the explicit forms [27,32] used in Ref. [1]:

$$\rho(r) = \rho_0 \frac{\sinh(c/a)}{\cosh(c/a) + \cosh(c/a)}, \quad (3)$$

with $\rho_0 = \frac{3}{4\pi c^3} \frac{1}{(1+(\pi b/c)^2)}$, c is the radius parameter and b represents the diffuseness. This density, denoted as the

symmetrized Fermi (SF) distribution, is normalized to unity. It differs from the usual Fermi function in that the exponential factor in the denominator is replaced by the hyperbolic cosine, and the two forms are identical in the limit that b goes to 0. This SF form allows an analytic Fourier transform so that the form factor, $F(q) = \int d^3r \rho(r) e^{-i\mathbf{q} \cdot \mathbf{r}}$, is given by

$$F(q) = \frac{4\pi^2 b c \rho_0}{q \sinh(\pi b q)} \left[\frac{\pi b}{c} \coth(\pi b q) \sin(qc) - \cos(qc) \right]. \quad (4)$$

Reference [1] used $c_p = 6.68$ fm and $a_p = 0.447$ fm, and extracted $c_n = 6.70$ fm and $a_n = 0.55$ fm. The form factors using $c_{p,n}$, $a_{p,n}$ are denoted as $F_{n,p}(q)$.

III. FINAL-STATE CHARGE EXCHANGE

This section examines the effect of charged pion production on one nucleon followed by a pion-nucleon charge exchange reaction on a second nucleon. See Fig. 1(b).

Computation requires knowledge of the photoproduction and the pion-nucleon scattering amplitudes. The amplitudes for $\gamma N \rightarrow \pi N$ have the general isospin structure $A = A^+ \delta_{b3} + A^- \frac{1}{2} [\tau_b, \tau_3] + A^0 \tau_b$. Only effects of the (3,3) resonance are included, and $A^{(3/2)} = A^+ - A^-$. Only A^- contributes to producing charged pions. This means the amplitude A^- is given by $A^- = -A^{(3/2)}$. The isospin structure of the πN scattering system is given by $T_{ba} = T^+ \delta_{ba} + \frac{1}{2} [\tau_b, \tau_a] T^-$, with only the term T^- (giving charge exchange) relevant here. Given these amplitudes as inputs, the diagrams of Fig. 1 may be evaluated.

A. S-wave final-state charge exchange

The two-body operator O_{ji}^S for a pion made on nucleon i to charge exchange via the S-wave on another nucleon j is given by

$$\begin{aligned} O_{ji}^S &= -\frac{A^{(3/2)}}{3} T^- e^{-i\mathbf{q} \cdot \mathbf{r}_j} 4\pi \int \frac{d^3q'}{(2\pi)^3} \frac{e^{i\mathbf{q}' \cdot (\mathbf{r}_j - \mathbf{r}_i)}}{q'^2 - q^2 + i\epsilon} I_F(j, i) \\ &\times \frac{2}{3} \hat{\mathbf{q}}'_{cN} \cdot (\hat{\mathbf{k}}_{cN} \times \boldsymbol{\epsilon}) e^{i\mathbf{k} \cdot \mathbf{r}_i}, \end{aligned} \quad (5)$$

with $I_F(j, i) = \boldsymbol{\tau}_i \cdot \boldsymbol{\tau}_j - \tau_3(j) \tau_3(i)$.

For the kinematics used here $\hat{\mathbf{q}}'_{cN} \approx \hat{\mathbf{q}}'$. This simplifies the expression so that the integral J given by

$$J = 4\pi \int \frac{d^3q'}{(2\pi)^3} \frac{e^{i\mathbf{q}' \cdot (\mathbf{r}_j - \mathbf{r}_i)}}{q'^2 - q^2 + i\epsilon} \hat{\mathbf{q}}' \cdot (\hat{\mathbf{k}}_{cN} \times \boldsymbol{\epsilon}) \quad (6)$$

is relevant. The use of rotational invariance shows that

$$J = \hat{\mathbf{r}}_{ji} \cdot (\hat{\mathbf{k}} \times \boldsymbol{\epsilon}) f(r) \quad (7)$$

with $\mathbf{r}_{ji} \equiv \mathbf{r}_j - \mathbf{r}_i$, and

$$f(r) = 4\pi \int \frac{d^3q'}{(2\pi)^3} \frac{e^{i\mathbf{q}' \cdot \mathbf{r}}}{q'^2 - q^2 + i\epsilon} \hat{\mathbf{q}}' \cdot \hat{\mathbf{r}}. \quad (8)$$

Evaluation of the integral gives

$$f(r) = \frac{-2i}{\pi r} + qj_1(qr) + \frac{2i}{\pi} \left(\frac{\text{Ci}(qr)[\sin(qr) - qr \cos(qr)] - \text{Si}(qr)[qr \sin(qr) + \cos(qr)] + qr}{qr^2} \right), \quad (9)$$

with Si and Ci being the standard sine and cosine integral functions. Putting everything together gives the resulting two-nucleon operator:

$$O_{ji}^S = \frac{2A^{(3/2)}}{9} T^- e^{-iq \cdot \mathbf{r}_j} I_F(j, i) f(r_{ji}) \hat{\mathbf{r}}_{ji} \cdot (\hat{\mathbf{k}} \times \boldsymbol{\epsilon}) e^{i\mathbf{k} \cdot \mathbf{r}_i}. \quad (10)$$

B. *P*-wave final-state charge exchange

There is a zero in forward-charge exchange on a nucleon that occurs at pion kinetic energies of about 50 MeV [33,34]. This corresponds to the kinetic energy of the pion produced by photons of energies of about 200 MeV. The amplitude T^- includes a *P*-wave term that can be expressed as

$$T_p^- = -T^- \hat{\mathbf{q}} \cdot \hat{\mathbf{q}}', \quad (11)$$

valid for values of q corresponding to the relevant pion kinetic energies. Then $T^- + T_p^- = 0$ for forward scattering at the appropriate energy. Including this *P*-wave final state charge exchange reaction leads to another $2N$ contribution denoted as O^P , given by the sum over i, j of

$$O_{ji}^P = + \frac{A^{(3/2)}}{3} T^- e^{-iq \cdot \mathbf{r}_j} 4\pi \times \int \frac{d^3 q'}{(2\pi)^3} \frac{e^{i\mathbf{q}' \cdot (\mathbf{r}_j - \mathbf{r}_i)}}{q'^2 - q^2 + i\epsilon} \hat{\mathbf{q}} \cdot \hat{\mathbf{q}}' I_F(i, j) \frac{2}{3} \hat{\mathbf{q}}' \cdot (\hat{\mathbf{k}} \times \boldsymbol{\epsilon}) e^{i\mathbf{k} \cdot \mathbf{r}_i} \quad (12)$$

Tensor correlations in the spin-0 nucleus can be ignored, so the integral may be simplified by doing the angle average over $\mathbf{r} \equiv \mathbf{r}_i - \mathbf{r}_j$. Then

$$O_{ji}^P = \frac{2A^{(3/2)}}{27} T^- e^{-iq \cdot \mathbf{r}_j} \hat{\mathbf{q}} \cdot (\hat{\mathbf{k}} \times \boldsymbol{\epsilon}) \frac{e^{iqr}}{r} e^{i\mathbf{k} \cdot \mathbf{r}_i}. \quad (13)$$

C. Nuclear matrix element

The coherent ground-state to ground-state matrix element must be evaluated. Define

$$O = \sum_{i \neq j} O_{ji}, \quad (14)$$

with $O_{ji} = O_{ji}^S + O_{ji}^P$. Use second quantization to get the result

$$\langle A|O|A \rangle = 2 \sum_{\alpha, \beta, \text{occupied}} \langle \alpha \beta | O_{12} (|\alpha \beta \rangle - |\beta \alpha \rangle). \quad (15)$$

Only the exchange term can contribute, as expected from the diagrams, so that

$$\langle A|O|A \rangle = -2 \sum_{\alpha, \beta, \text{occupied, np}} \langle \alpha \beta | \tilde{O}_{12} | \beta \alpha \rangle. \quad (16)$$

There are two terms because either α or β can denote a neutron, with the other being a proton. The net result is

$$\langle A|O^S|A \rangle = -2 \frac{A^{3/2}}{3} T^- \frac{2}{3} \int d^3 r_1 d^3 r_2 e^{-iq \cdot \mathbf{r}_2} \rho_n(\mathbf{r}_2, \mathbf{r}_1) \times \rho_p(\mathbf{r}_1, \mathbf{r}_2) e^{i\mathbf{k} \cdot \mathbf{r}_1} f(r_{12}) \hat{\mathbf{r}}_{21} \cdot (\hat{\mathbf{k}} \times \boldsymbol{\epsilon}), \quad (17)$$

and

$$\langle A|O^P|A \rangle = -2 \frac{A^{3/2}}{3} T^- \frac{2}{9} \int d^3 r_1 d^3 r_2 e^{-iq \cdot \mathbf{r}_2} \rho_n(\mathbf{r}_2, \mathbf{r}_1) \times \rho_p(\mathbf{r}_1, \mathbf{r}_2) e^{i\mathbf{k} \cdot \mathbf{r}_1} \frac{e^{iqr_{12}}}{r_{12}} \hat{\mathbf{q}} \cdot (\hat{\mathbf{k}} \times \boldsymbol{\epsilon}). \quad (18)$$

The term $\rho_{n(p)}(\mathbf{r}_2, \mathbf{r}_1)$ is the neutron (n) or proton (p) density matrix given by

$$\rho_{n(p)}(\mathbf{r}_2, \mathbf{r}_1) \equiv \sum_{\alpha} c_{n(p)}^{\alpha} \phi_{\alpha}^*(\mathbf{r}_2) \phi_{\alpha}(\mathbf{r}_1), \quad (19)$$

where α represents the given orbital and $c_{n(p)}^{\alpha}$ represents the occupation number. The density matrices are evaluated using a local density approximation according to Negele and Vautherin [35]. Defining $\mathbf{R} \equiv \frac{1}{2}(\mathbf{r}_1 + \mathbf{r}_2)$, $\mathbf{r} \equiv \mathbf{r}_1 - \mathbf{r}_2$ one has

$$\rho_v(\mathbf{r}_1, \mathbf{r}_2) \approx \rho_v(R) P_v(r), \quad (20)$$

with $P_v(r) \equiv \frac{3j_1(k_{Fv}r)}{k_{Fv}r}$ and v refers to n, p . Then

$$\langle A|O^S|A \rangle = -2 \frac{A^{3/2}}{3} T^- \frac{2}{3} \int d^3 R d^3 r e^{-i(\mathbf{q}-\mathbf{k}) \cdot \mathbf{R}} \rho_n(\mathbf{R}) \rho_p(\mathbf{R}) \times e^{i(\mathbf{q}+\mathbf{k}) \cdot \mathbf{r}/2} f(r) P_n(r) P_p(r) \hat{\mathbf{r}} \cdot (\hat{\mathbf{k}} \times \boldsymbol{\epsilon}) \quad (21)$$

The angular integral over $\hat{\mathbf{r}}$ is handled first using [with $\mathbf{V} \equiv \frac{1}{2}(\mathbf{q} + \mathbf{k})$] The necessary integral is given by $\int d\hat{\mathbf{r}} e^{i\mathbf{V} \cdot \mathbf{r} \hat{\mathbf{r}}} = i\sqrt{V} 4\pi j_1(Vr)$. Then

$$\langle A|O^S|A \rangle = -\frac{2i\pi}{9} A^{(3/2)} T^- \int d^3 R e^{-i(\mathbf{q}-\mathbf{k}) \cdot \mathbf{R}} \rho_n(\mathbf{R}) \rho_p(\mathbf{R}) \times \int r^2 dr j_1(Vr) f(r) P_n(r) P_p(r) \frac{\mathbf{q}}{V} \cdot (\hat{\mathbf{k}} \times \boldsymbol{\epsilon}), \quad (22)$$

and

$$\langle A|O^P|A \rangle = -\frac{4i\pi}{27} A^{(3/2)} T^- \int d^3 R e^{-i(\mathbf{q}-\mathbf{k}) \cdot \mathbf{R}} \rho_n(\mathbf{R}) \rho_p(\mathbf{R}) \times \int r^2 dr j_0(Vr) P_n(r) P_p(r) \frac{e^{iqr}}{r} \hat{\mathbf{q}} \cdot (\hat{\mathbf{k}} \times \boldsymbol{\epsilon}). \quad (23)$$

Both of the two-body amplitudes depend on the Fourier transform of the product of neutron and proton densities, $F_2(q) = \int d^3 r \rho^2(r) e^{-iq \cdot \mathbf{r}}$, is presented for comparison

purposes. It given by:

$$F_2(q) = \frac{(2\pi\rho_0 b)^2 \left[\cos(cq) \left(1 - \frac{c \coth(\frac{c}{b})}{b} - \pi b q \coth(\pi b q) \right) + \sin(cq) \left(\pi \coth(\frac{c}{b}) \coth(\pi b q) - cq \right) \right]}{q \sinh(\pi b q)}. \quad (24)$$

The Fourier transform of the product of the neutron and proton densities can be obtained to better than about a tenth of a percent, for relevant values of the momentum transfer, by using the geometric mean of the neutron and proton radius and diffuseness parameters in the above equation.

The complete scattering amplitude, \mathcal{M} is obtained by summing the terms of Eqs. (2), (22), and (23) so that

$$\mathcal{M} = \langle A | O^{IA} + O^S + O^P | A \rangle. \quad (25)$$

This amplitude is squared, and with the appropriate factors used to compute the cross section.

IV. NONZERO EXTENT OF THE PROTON

Electron scattering determines the charge nuclear charge density. Computing the (γ, π^0) cross section requires the input of the point proton charge density. Reference [1] obtained this density by using parameters from Klos *et al.* [36] who refer to the charge distribution of Fricke *et al.* [37], together with an approximation given by Oset *et al.* [38] to transform the charge-density parameters to those for point protons based on taking into account the proton finite size. This approximation is applicable only if $q^2 R_A^2 \ll 1$. The relevant momentum transfer here is between 0.3 and 0.9 fm⁻¹ so that $q^2 R_A^2$ ranges between about 5 and 50. This feature was noted by [31] who provided two-parameter Fermi (2PF) function fits to experimental charge and point-proton density. However, the density used in Ref. [1] is a symmetrized 2PF function. The symmetrized Fermi density is given by [27,32] Eq. (3) and form factor given by Eq. (4).

The effects of the spatial extent of the proton's charge density are reassessed here. The point-proton form factor is usually taken as the nuclear charge form factor $F_A(q) = \int d^3r e^{i\mathbf{q}\cdot\mathbf{r}} \rho_A(r)$ divided by $G_E(q)$, the Sachs electric form factor of the proton. Thus the point proton form factor is

$$F_{\text{pt}}(q) = \frac{F_A(q)}{G_E(q)}, \quad (26)$$

with $F_A(q) = NF_n(q) + ZF_p(q)$. Corrections to Eq. (26) are studied in Ref. [39], but are not included here because the

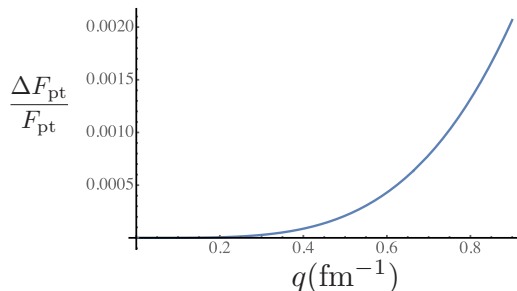


FIG. 2. The form factors of Eq. (26) (solid) and Eq. (28) (dashed).

entire effect of the proton size is already known to be small. The dipole parametrization

$$G_E(q^2) = \frac{1}{(1 + q^2/\Lambda^2)^2} \quad (27)$$

generally represents the data very well in the region with $q \leq 0.9$ fm⁻¹, which corresponds to $q^2 \leq 0.04$ GeV². The exact value of Λ is currently in dispute [29,30]. A value of $\Lambda = 3.93$ fm⁻¹ is used here that corresponds to a proton radius of 0.84 fm.

The approximation used previously corresponds to obtaining the correct mean-square radius so that the resulting point form factor $\tilde{F}_{\text{pt}}(q)$ is given by

$$\tilde{F}_{\text{pt}}(q) = (1 + 2q^2/\Lambda^2)F_A(q). \quad (28)$$

The difference between the exact and approximate form factors is $\Delta F_{\text{pt}}(q) \equiv F_{\text{pt}}(q) - \tilde{F}_{\text{pt}}(q)$ and $\Delta F_{\text{pt}}(q)/F_{\text{pt}}(q)$ is displayed in Fig 2. The very small values obtained validate the treatment of Ref. [1]. The tiny correction $\Delta F_{\text{pt}}(q)$ is ignored in the following treatment.

V. ANALYSIS AND RESULT FOR THE NEUTRON SKIN

The first step is to show the size of the two-body effects: Fig. 3. The red dashed curve reproduces the plane wave calculation shown in Ref. [1].¹ Figure 4 shows the fractional change in the cross section. The effects of the two-body term increase the cross section by about 6% at the first maximum and by about 5% at the second maximum. Including the effects of final-state charge exchange causes the position of the minimum to be increased by only about 0.001 fm⁻¹. This shift is ignorable, but as a result of this difference, the changes obtain very large magnitudes for values of Δq near the minimum.

The next step is to assess how including the two-body terms of Fig. 1 impact the extracted value of the neutron skin. To do this, the cross section obtained from the one-body mechanism with the density parameters of Ref. [1] is taken as representing the data. Then the complete calculation that includes the charge exchange effect is computed as a function of new values of a_n . Values of a_n are varied to find a value that causes the full calculation (including one- plus two-body amplitudes) is the same as the data. The result is shown in Fig. 5. Using $a_n = 0.61$ fm instead 0.55 fm in the full calculation leads to a reproduction of the data. In Fig. 5 the solid blue (complete calculation) curve of that overlaps the red dashed (one-body only) nearly completely. Differences are generally much, much smaller than the 3% error assigned to the data in Ref. [1].

¹The label of the ordinate axis of Fig. 2 of Ref. [1] is missing a factor of $\sin \theta$.

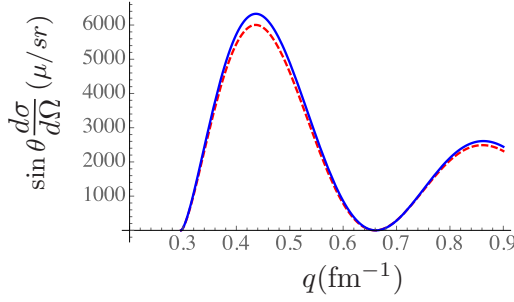


FIG. 3. Cross section as a function of momentum transfer $\Delta q \equiv |\mathbf{k} - \mathbf{q}|$. Solid (blue) is the complete calculation including the one-body and two-body terms. Dashed (red) includes one-body only.

Given the new values of a_n and c_n one may compute the neutron skin. The rms radius R for a symmetrized Fermi distribution of radius c and diffuseness a is given by the expression:

$$R = \sqrt{\frac{1}{5}(3c^2 + 7\pi^2 a^2)}. \quad (29)$$

Using $c_p = 6.68$ fm and $a_p = 0.447$ gives $R_p = 5.43$ fm. Using the values $c_n = 6.70$ fm and $a_n = 0.55$ fm of Ref. [1] gives $R_n = 5.58$ fm, and a skin,

$$\Delta r_{np} \equiv R_n - R_p, \quad (30)$$

of 0.143 fm consistent with the result of that reference. Using instead $a_n = 0.61$ fm and $c_n = 6.7$ fm, which takes the effect of final-state charge exchange into account, leads to $R_n = 5.79$ fm and a neutron skin of 0.229 fm. The effects of final-state charge exchange are not included in the extraction of the neutron skin reported by Ref. [1]. Including these effects here leads to an increase of the neutron skin by about 50%. The same neutron skin is obtained by increasing the value of c_n by about 0.10 fm.

The experimental analysis [1] did not use the absolute cross section in extracting the neutron skin, so that the fits in each bin of photon energy have a free normalization parameter. The theoretical model reproduced the data within 5–10% for all bins of the photon energy. The 5–10% differences between the theory and experiment are not reflected in the figures in the paper.

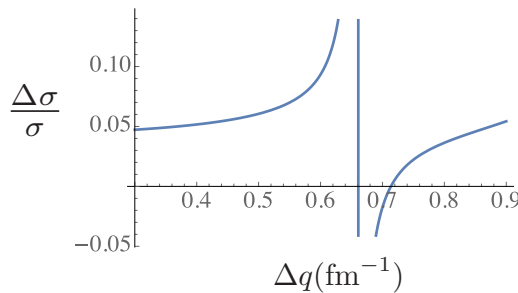


FIG. 4. Fractional change of the cross section $\Delta\sigma$ caused by including the charge exchange final-state interaction as a function of momentum transfer $\Delta q \equiv |\mathbf{k} - \mathbf{q}|$.

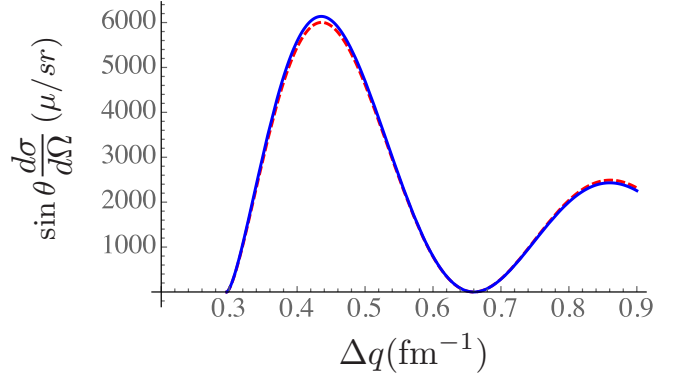


FIG. 5. Cross section as a function of momentum transfer q . Solid (blue) is the complete calculation including the one-body and two-body terms. Dashed (red) includes one-body only with $a_n = 0.61$ fm

Changing the normalization to match the data to the theory represents one of the errors in the theory. Here the analogous treatment would be to multiply the first (IA) term of Eq. (25) by the necessary constant needed to reproduce the data. As a result the both the theory and the data are represented by the impulse approximation. Suppose a normalization factor of $\mathcal{N} \approx 1$ is needed to match theoretically computed cross section to the data. This means that the impulse approximation term of Eq. (25) would be multiplied by $\sqrt{\mathcal{N}}$. Then the influence of the final-state charge exchange amplitudes would be changed by only a factor of $\sqrt{\mathcal{N}} - 1$. For example, increasing the computed cross section by, e.g., 5% to reproduce the means that the amplitude O^{IA} would be changed by a factor of about 1.025. The renormalized calculation would then be represented by multiplying the first term O^{IA} of Eq. (25) by 1.025. Then the relative importance of the charge exchange terms, $O^S + O^P$, is reduced only by 2.5%. The 6% increase in the peak cross section reported above would be changed to an increase of 5.85%. The change would truly be negligible. If $\mathcal{N} < 1$ the importance of the final-state charge exchange amplitudes would be increased. Thus, any uncertainty in normalization has no impact on the present conclusion that the neutron skin could be 50% larger than the reported value.

Moreover, the theory predicts a significant rise in the cross section as the photon energy rises from 180–240 MeV because the energy approaches that of the Δ peak. The floating normalization procedure used in Ref. [1] loses the opportunity to precisely test the theory.

VI. SUMMARY AND DISCUSSION

The present effort treats two specific corrections to the reaction mechanism used to extract the neutron density. The effect of charge exchange in the final state leads to a significant (50%) computed increase in the extracted neutron skin. The effects of the proton's charge density are correctly handled in Ref. [1].

But there are many other uncertainties associated with the pion-nucleus final-state interaction that have not been treated here or in Ref. [1]. The pion-nucleus optical potential, nec-

essary to analyze data for photon energies higher than treated here does not determine pion wave function within the nuclear interior. The resulting ambiguities have long been known to lead to significant uncertainties in computing reaction cross sections [40,41]. Moreover, the optical potential [27] used by Ref. [1] was constrained only by nuclei with equal numbers of neutrons and protons. In particular, the optical potential was not tested by comparing to pion-Pb elastic scattering data. A key element in the optical potential is the Δ -nuclear interaction, but no consensus was ever reached on that interaction [42–44].

Another issue is that of off-shell effects in the pion-nucleon interaction. The pion-nucleon interaction of Eq. (11) has been instead written as

$$T_p^- = -\hat{T}^- \mathbf{q} \cdot \mathbf{q}' \quad (31)$$

because \hat{T}^- is independent of energy at the low pion energies relevant here. The scattering amplitudes of Eqs. (11) and (31) are the same for on energy-shell kinematic conditions, but differ when $|\mathbf{q}'| \neq |\mathbf{q}|$. Including this effect increases the amplitude O^P by at least 30%. A detailed analysis of pion-nucleus elastic scattering data shows that the form of Eq. (31) reproduced all of the systematic features of the data [45].

Other issues involve potential differences between the reaction theories of Refs. [18,22] and the sensitivity of any theory

to uncertainties in the γ -nucleon interaction that are input to the reaction theory. Treating such problems is far beyond the scope of the present effort, but the discussed previous experience suggests that the related uncertainties are rather large compared to the precision that is relevant for extracting the neutron skin.

All of these considerations make it clear that there is a substantial systematic error arising from uncertainties in the theoretical model used to compute the (γ, π^0) cross section that was not taken into account in Ref. [1]. Given only the size of the effects of the diagrams of Fig. 1(b), one can confidently assert that the total (experimental plus theoretical) systematic error was underestimated by at least a factor of three. Including the effects of final-state charge exchange along with the uncertainties discussed in the present section suggest that the result for the neutron skin could be written as

$$\Delta r_{np} = 0.23 \pm 0.03 \text{ (stat.)}_{-0.03}^{+0.02} \text{ (sys.)} \pm 0.07 \text{ (th.sys.) fm.} \quad (32)$$

ACKNOWLEDGMENTS

This work has been partially supported by the US Department of Energy Office of Science, Office of Nuclear Physics under Award No. DE-FG02-97ER-41014.

-
- [1] C. M. Tarbert *et al.*, Neutron Skin of ^{208}Pb from Coherent Pion Photoproduction, *Phys. Rev. Lett.* **112**, 242502 (2014).
- [2] A. W. Steiner, M. Prakash, J. M. Lattimer, and P. J. Ellis, Isospin asymmetry in nuclei and neutron stars, *Phys. Rep.* **411**, 325 (2005).
- [3] C. J. Horowitz and J. Piekarewicz, Neutron Star Structure and the Neutron Radius of ^{208}Pb , *Phys. Rev. Lett.* **86**, 5647 (2001).
- [4] J. Xu, L.-W. Chen, B.-A Li, and H.-R. Ma, Nuclear constraints on properties of neutron star crusts, *Astrophys. J.* **697**, 1549 (2009).
- [5] A. W. Steiner, J. M. Lattimer, and E. F. Brown, The equation of state from observed masses and radii of neutron stars, *Astrophys. J.* **722**, 33 (2010).
- [6] B. G. Todd-Rutel and J. Piekarewicz, Neutron-Rich Nuclei and Neutron Stars: A New Accurately Calibrated Interaction for the Study of Neutron-Rich Matter, *Phys. Rev. Lett.* **95**, 122501 (2005).
- [7] D. H. Wen, B. A. Li, and L. W. Chen, Super-Soft Symmetry Energy Encountering Non-Newtonian Gravity in Neutron Stars, *Phys. Rev. Lett.* **103**, 211102 (2009).
- [8] S. J. Pollock and M. C. Welliver, Effects of neutron spatial distributions on atomic parity nonconservation in cesium, *Phys. Lett. B* **464**, 177 (1999).
- [9] M. B. Tsang, J. R. Stone, F. Camera, P. Danielewicz, S. Gandolfi, K. Hebeler, C. J. Horowitz, J. Lee, W. G. Lynch, Z. Kohley, R. Lemmon, P. Moller, T. Murakami, S. Riordan, X. Roca-Maza, F. Sammarruca, A. W. Steiner, I. Vidana, and S. J. Yennello, Constraints on the symmetry energy and neutron skins from experiments and theory, *Phys. Rev. C* **86**, 015803 (2012).
- [10] K. Hebeler, J. M. Lattimer, C. J. Pethick, and A. Schwenk, Constraints on Neutron Star Radii Based on Chiral Effective Field Theory Interactions, *Phys. Rev. Lett.* **105**, 161102 (2010).
- [11] M. Centelles, X. Roca-Maza, X. Viñas, and M. Warda, Nuclear Symmetry Energy Probed by Neutron Skin Thickness of Nuclei, *Phys. Rev. Lett.* **102**, 122502 (2009).
- [12] A. Carbone, G. Colo, A. Bracco, L. G. Cao, P. F. Bortignon, F. Camera, and O. Wieland, Constraints on the symmetry energy and on neutron skins from the pygmy resonances in ^{68}Ni and ^{132}Sn , *Phys. Rev. C* **81**, 041301(R) (2010).
- [13] L. W. Chen, C. M. Ko, B. A. Li, and J. Xu, Density slope of the nuclear symmetry energy from the neutron skin thickness of heavy nuclei, *Phys. Rev. C* **82**, 024321 (2010).
- [14] A. Tamii *et al.*, Complete Electric Dipole Response and the Neutron Skin in ^{208}Pb , *Phys. Rev. Lett.* **107**, 062502 (2011).
- [15] B. A. Li, L. W. Chen, and C. M. Ko, Recent progress and new challenges in isospin physics with heavy-ion reactions, *Phys. Rep.* **464**, 113 (2008).
- [16] M. B. Tsang, Y. Zhang, P. Danielewicz, M. Famiano, Z. Li, W. G. Lynch, and A. W. Steiner, Constraints On the Density Dependence of the Symmetry Energy, *Phys. Rev. Lett.* **102**, 122701 (2009).
- [17] J. Piekarewicz and F. J. Fattoyev, Neutron-rich matter in heaven and on earth, *Phys. Today* **72**, 30 (2019).
- [18] D. Drechsel, L. Tiator, S. S. Kamalov, and S. N. Yang, Medium effects in coherent pion photoproduction and electroproduction on ^4He and ^{12}C , *Nucl. Phys. A* **660**, 423 (1999).

- [19] D. Drechsel, O. Hanstein, S. S. Kamalov, and L. Tiator, A Unitary isobar model for pion photoproduction and electroproduction on the proton up to 1-GeV, *Nucl. Phys. A* **645**, 145 (1999).
- [20] B. Krusche, J. Ahrens, R. Beck, S. Kamalov, V. Metag, R. O. Owens, and H. Stroher, Coherent π^0 photoproduction from atomic nuclei, *Phys. Lett. B* **526**, 287 (2002).
- [21] B. Krusche, Nuclear mass form-factors from coherent photoproduction of π^0 mesons, *Eur. Phys. J. A* **26**, 7 (2005).
- [22] W. Peters, H. Lenske, and U. Mosel, Coherent photoproduction of pions on nuclei in a relativistic, nonlocal model, *Nucl. Phys. A* **640**, 89 (1998).
- [23] T. E. O. Ericson and W. Weise, *Pions and Nuclei* (Clarendon Press, Oxford, 1988).
- [24] G. Faldt, The pion mass difference in threshold pion reactions on light nuclei, *Nucl. Phys. A* **333**, 357 (1980).
- [25] P. Argan *et al.*, Analysis of π^0 photoproduction measurements near threshold on light nuclei, *Phys. Rev. C* **24**, 300 (1981).
- [26] P. Wilhelm and H. Arenhövel, Rescattering effects in coherent pion photoproduction on the deuteron in the Delta resonance region, *Nucl. Phys. A* **609**, 469 (1996).
- [27] M. Gmitro, S. S. Kamalov, and R. Mach, Momentum space second order optical potential for pion nucleus elastic scattering, *Phys. Rev. C* **36**, 1105 (1987).
- [28] D. Drechsel and L. Tiator, Threshold pion photoproduction on nucleons, *J. Phys. G* **18**, 449 (1992).
- [29] R. Pohl, R. Gilman, G. A. Miller, and K. Pachucki, Muonic hydrogen and the proton radius puzzle, *Ann. Rev. Nucl. Part. Sci.* **63**, 175 (2013).
- [30] C. E. Carlson, The proton radius puzzle, *Prog. Part. Nucl. Phys.* **82**, 59 (2015).
- [31] A. B. Jones and B. A. Brown, Two-parameter Fermi function fits to experimental charge and point-proton densities for ^{208}Pb , *Phys. Rev. C* **90**, 067304 (2014).
- [32] A. A. Chumalov, R. A. Eramzhian, and S. S. Kamalov, Dwia in the momentum space for (γ, π^0) reaction near threshold, *Z. Phys. A* **328**, 195 (1987).
- [33] D. H. Fitzgerald *et al.*, Forward angle cross-sections for pion nucleon charge exchange between 100-MeV/c and 150-MeV/c, *Phys. Rev. C* **34**, 619 (1986).
- [34] F. Irom, M. J. Leitch, H. W. Baer, J. D. Bowman, M. D. Cooper, B. J. Dropesky, E. Piasetzky, and J. N. Knudson, Energy And Mass Dependence Of Low-energy Pion Single Charge Exchange To The Isobaric Analog State, *Phys. Rev. Lett.* **55**, 1862 (1985).
- [35] J. W. Negele and D. Vautherin, Density-matrix expansion for an effective nuclear Hamiltonian. II, *Phys. Rev. C* **11**, 1031 (1975).
- [36] B. Klos *et al.*, Neutron density distributions from antiprotonic ^{208}Pb and ^{209}Bi atoms, *Phys. Rev. C* **76**, 014311 (2007).
- [37] G. Fricke, C. Bernhardt, K. Heilig, L. A. Schaller, L. Schellenberg, E. B. Shera, and C. W. de Jager, Nuclear Ground State Charge Radii from Electromagnetic Interactions, *Atom. Data Nucl. Data Tabl.* **60**, 177 (1995).
- [38] E. Oset, P. Fernandez de Cordoba, L. L. Salcedo, and R. Brockmann, Decay Modes of Σ and Λ Hypernuclei, *Phys. Rept.* **188**, 79 (1990).
- [39] G. A. Miller, Confinement in nuclei and the expanding proton, [arXiv:1907.00110](https://arxiv.org/abs/1907.00110) [nucl-th].
- [40] G. A. Miller, Positive pion production by 185 MeV protons, *Nucl. Phys. A* **224**, 269 (1974); **235**, 531(E) (1974).
- [41] B. D. Keister, Phase shift equivalent potentials and pion-nucleus reactions, *Phys. Rev. C* **18**, 1934 (1978).
- [42] E. Oset and W. Weise, Elastic scattering of pions from ^{16}O in the isobar hole model, *Nucl. Phys. A* **329**, 365 (1979).
- [43] M. Hirata, J. H. Koch, E. J. Moniz, and F. Lenz, Isobar-hole doorway states and $\pi-^{16}\text{O}$ scattering, *Ann. Phys. (NY)* **120**, 205 (1979).
- [44] R. A. Freedman, G. A. Miller, and E. M. Henley, Isobar dynamics and pion nucleus elastic scattering, *Nucl. Phys. A* **389**, 457 (1982).
- [45] E. Friedman, Systematics of pion - nucleus optical potentials from analysis of elastic scattering, *Phys. Rev. C* **28**, 1264 (1983).